J|A|C|S
ARTICLES
Published on Web 05/11/2007

Pyromellitamide Aggregates and Their Response to Anion Stimuli

James E. A. Webb, Maxwell J. Crossley, Peter Turner, and Pall Thordarson*

Contribution from the School of Chemistry, The University of Sydney NSW 2006, Australia

Received February 27, 2007; E-mail: p.thordarson@chem.usyd.edu.au

Abstract: The *N*,*N*′,*N*″,*N*‴-1,2,4,5-tetra(ethylhexanoate) pyromellitamide is found to be capable of both intermolecular aggregation and binding to small anions. It is synthesized by aminolysis of pyromellitic anhydride with ethanolamine, followed by a reaction with hexanoyl chloride. The single-crystal X-ray structure of the pyromellitamide shows that it forms one-dimensional columnar stacks through an intermolecular hydrogen-bonding network. It also forms self-assembled gels in nonpolar solvents, presumably by a hydrogen-bonding network similar to the solid-state structure as shown by IR and XRD studies. Aggregation by intermolecular hydrogen bonding of the pyromellitamide is also observed by NMR and IR in solution. Fitting of NMR dilution data for pyromellitamide in d_6-acetone to a cooperative aggregation model gave $K_E = 232\ M^{-1}$ and positive cooperativity of aggregation ($\rho = 0.22$). The pyromellitamide binds to a range of small anions with the binding strength decreasing in the order chloride > acetate > bromide > nitrate ≈ iodide. The data indicate that the pyromellitamide binds two anions and that it displays negative cooperativity. The intermolecular aggregation of the pyromellitamide can also be altered using small anion stimuli; anion addition to preformed self-assembled pyromellitamide gels causes their collapse. The kinetics of anion-induced gel collapse are qualitatively correlated to the binding affinities of the same anions in solution. The cooperative anion binding properties and the sensitivity of the self-assembled gels formed by pyromellitamide toward anions could be useful in the development of sensors and switching/releasing devices.

Introduction

Stimuli responsive biological systems provide some of the most elegant demonstrations of the importance of supramolecular interactions in nature. A well-known example is the cooperative binding of small ligands to multivalent hosts, as in the case of allosteric[1] oxygen binding to hemoglobin,[2] where successive binding of the ligand(s) changes the structure and/or function of the host in a nonlinear fashion. External stimuli can also be used to influence intermolecular interactions as in the case of self-assembled protein filaments, where the structure can be modulated in vivo and in vitro with various small-molecule effectors. For instance, iodide is known to cause the depolymerization (collapse) of actin filaments (F-actin)[3] and the corresponding transition from a gel-like to solution state (gel → sol transition), possibly by influencing the unique hydration shell that is thought to surround and stabilize the F-actin polymer.[4]

Much effort has been directed toward mimicking biological systems that respond to external stimuli. There are numerous examples of simple synthetic allosteric host−guest systems.[5,6] The vast majority of these concern the use of cationic or neutral guests (effectors), while relatively few discrete multivalent hosts displaying cooperative binding toward anions have been reported.[6c,7] The intermolecular interactions of synthetic self-assembled systems, including macroscopic self-assembled molecular gels,[8] can also be tuned using small ionic or molecular effectors. Self-assembled molecular gels are showing increased potential for applications in biomedicine for drug delivery[9] and in tissue engineering[10] (e.g., by stimulating nerve regrowth in spinal injuries).[11] To date, there have been reports on molecular

(1) (a) Monod, J.; Changeux, J.-P.; Jacob, F. *J. Mol. Biol.* **1963**, *6*, 306. (b) Monod, J.; Wyman, J.; Changeux, J.-P. *J. Mol. Biol.* **1965**, *12*, 88.
(2) (a) Ackers, G. K.; Doyle, M. L.; Myers, D.; Daugherty, M. A. *Science* **1992**, *255*, 54. (b) Huang, Y.; Doyle, M. L.; Ackers, G. K. *Biophys. J.* **1996**, *71*, 2094. (c) Johnson, M. L. *Methods Enzymol.* **2000**, *323*, 124.
(3) (a) Straub, F. B. *Stud. Inst. Med. Chem. Univ. Szeged* **1942**, *2*, 4. (b) Straub, F. B. *Stud. Inst. Med. Chem. Univ. Szeged* **1942**, *2*, 7. (c) Guba, F. *Nature* **1950**, *165*, 439.
(4) Kabir, S. R.; Yokoyama, K.; Mihashi, K.; Kodama, T. *Biophys. J.* **2003**, *85*, 3154.
(5) For reviews, see: (a) Rebek, J., Jr. *Acc. Chem. Res.* **1984**, *17*, 258. (b) Shinkai, S.; Ikeda, M.; Sugasaki, A.; Takeuchi, M. *Acc. Chem. Res.* **2001**, *34*, 494. (c) Takeuchi, M.; Ikeda, M.; Sugasaki, A.; Shinkai, S. *Acc. Chem. Res.* **2001**, *34*, 865. (d) Kovbasyuk, L.; Krämer, R. *Chem. Rev.* **2004**, *104*, 3161.
(6) For some recent examples, see: (a) Thordarson, P.; Bijsterveld, E. J. A.; Elemans, J. A. A. W.; Kasák, P.; Nolte, R. J. M.; Rowan, A. E. *J. Am. Chem. Soc.* **2003**, *125*, 1186. (b) Thordarson, P.; Coumans, R. G. E.; Elemans, J. A. A. W.; Thomassen, P. J.; Visser, J.; Rowan, A. E.; Nolte, R. J. M. *Angew. Chem., Int. Ed.* **2004**, *43*, 4755. (c) Hirata, O.; Takeuchi, M.; Shinkai, S. *Chem. Commun.* **2005**, 3805. (d) Wakabayashi, R.; Kubo, Y.; Hirata, O.; Takeuchi, M.; Shinkai, S. *Chem. Commun.* **2005**, 5742. (e) Thomassen, P. J.; Foekema, J.; Jordana, i Lluch, R.; Thordarson, P.; Elemans, J. A. A. W.; Nolte, R. J. M.; Rowan, A. E. *New. J. Chem.* **2006**, *30*, 148. (f) Sessler, J. L.; Tomat, E.; Lynch, V. M. *J. Am. Chem. Soc.* **2006**, *128*, 4184. (g) Ikeda, T.; Hirata, O.; Takeuchi, M.; Shinkai, S. *J. Am. Chem. Soc.* **2006**, *128*, 16008. (h) Heo, J.; Mirkin, C. A. *Angew. Chem., Int. Ed.* **2006**, *45*, 941.
(7) Apart from ref 6c, the only neutral non-metallic hosts that show cooperative binding toward anions are fluoride receptors such as: (a) Kavallieratos, K.; Bertao, C. M.; Crabtree, R. H. *J. Org. Chem.* **1999**, *64*, 1675. Examples of organometallic hosts showing cooperative binding to anions other than fluoride include: (b) Uppadine, L. H.; Drew, M. G. B.; Beer, P. D. *Chem. Commun.* **2001**, 291. (c) Lazarides, T.; Miller, T. A.; Jeffery, J. C.; Ronson, T. K.; Adams, H.; Ward, M. D. *Dalton Trans.* **2005**, 528. (d) Kim, D.-S.; Miyaji, H.; Chang, B.-Y.; Park, S.-M.; Ahn, K. H. *Chem. Commun.* **2006**, 3314.

Chart 1

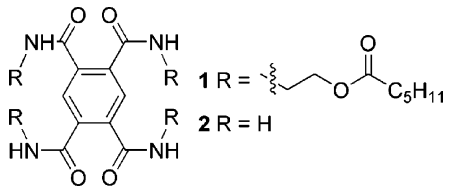

gels that are responsive to pH changes,[12a] light,[12b,c] catalysis (both chemical[12d] and enzymatic[12e−g]), and cation recognition.[12h,i] The use of metal salts (e.g., $AgBF_4$) has also been found to template the formation of a gel from a simple bis(urea) compound and the anion shown to influence the gel structure by hydrogen-bonding interactions.[13] Prior to this work, however, there has only been one communication of using anions to inhibit the formation of self-assembled molecular gels.[14] This is somewhat surprising, as many low-molecular mass organic gelators (LMOG),[8] that is, compounds that form self-assembled gels, aggregate by the virtue of bis-urea groups or amide groups often found in anion receptors. Among amide-based anion receptors, the isophthalamides[15] were the first acyclic anion receptor to gain popularity in supramolecular chemistry and are now one of the most heavily used in this area of research.[7a,16] To date, however, there have been no reports of a ditopic version of this receptor, or to the best of our knowledge, no reports on self-assembled gels based on this class of molecules.

We report herein the synthesis of *N*,*N*′,*N*″,*N*‴-1,2,4,5-tetra-(ethylhexanoate) pyromellitamide **1** (Chart 1). Remarkably, although the parent pyromellitamide **2** has been known since 1914,[17] there are not many reports of pyromellitamides in the literature[18] and no reports regarding their supramolecular properties. The pyromellitamides can be viewed structurally as the ditopic version of the isophthalamides. The pyromellitamide **1** reported here displays aggregation behavior, including gel formation, and binds to anions with a 1:2 host/anion stoichiometry and negative cooperativity. The ability of pyromellitamide **1** to form self-assembled gels is not unexpected as it fits well within the "rigid core/flexible tail" motif,[8,19] commonly found among other LMOG, being composed of a rigid aromatic core with four amides linked to four flexible ethyl hexanoate tails. The gels formed by **1** respond to the addition of anions, by collapsing back to the solution state (anion-induced gel → sol transition).

Scheme 1. Synthesis of **1**

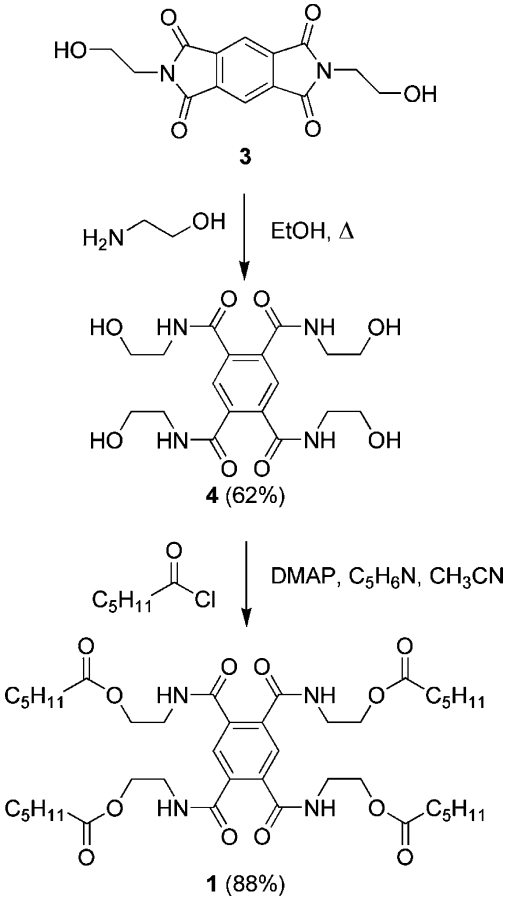

Results and Discussion

Synthesis and Solid-State Structure of Pyromellitamide 1. The pyromellitamide **1** was synthesized in two steps by the

(8) For reviews, see: (a) Terech, P.; Weiss, R. G. *Chem. Rev.* **1997**, *97*, 3133. (b) Abdallah, D. J.; Weiss, R. G. *Adv. Mater.* **2000**, *12*, 1237. (c) van Esch, J. H.; Feringa, B. L. *Angew. Chem., Int. Ed.* **2000**, *39*, 2263. (d) Estroff, L. A.; Hamilton, A. D. *Chem. Rev.* **2004**, *104*, 1201. (e) Hirst, A. R.; Smith, D. K. *Chem.−Eur. J.* **2005**, *11*, 5496. (f) de Loos, M.; Feringa, B. L.; van Esch, J. H. *Eur. J. Org. Chem.* **2005**, 3615. (g) George, M.; Weiss, R. G. *Acc. Chem. Res.* **2006**, *39*, 489.

(9) (a) Xing, B. G.; Yu, C. W.; Chow, K. H.; Ho, P. L.; Fu, D. G.; Xu, B. *J. Am. Chem. Soc.* **2002**, *124*, 14846. (b) Motulsky, A.; Lafleur, M.; Couffin-Hoarau, A.-C.; Hoarau, D.; Boury, F.; Beonit, J.-P.; Leroux, J.-C. *Biomaterials* **2005**, *26*, 6242−6253.

(10) Rajangam, K.; Behanna, H. A.; Hui, M. J.; Han, X.; Hulvat, J. F.; Lomasney, J. W.; Stupp, S. I. *Nano Lett.* **2006**, *6*, 2086.

(11) Silva, G. A.; Czeisler, C.; Niece, K. L.; Beniash, E.; Harrington, D. A.; Kessler, J. A.; Stupp, S. I. *Science* **2004**, *303*, 1352.

(12) For some representative examples, see: (a) Pozzo, J.-L.; Clavier, G. M.; Desvergne, J.-P. *J. Mater. Chem.* **1998**, *8*, 2575. (b) Murata, K.; Aoki, M.; Nishi, T.; Ikeda, A.; Shinkai, S. *J. Chem. Soc., Chem. Commun.* **1991**, 1715. (c) Murata, K.; Aoki, M.; Suzuki, T.; Harada, T.; Kawabata, H.; Komori, T.; Ohseto, F.; Ueda, K.; Shinkai, S. *J. Am. Chem. Soc.* **1994**, *116*, 6664. (d) Love, C. S.; Chechik, V.; Smith, D. K.; Ashworth, I.; Brennan, C. *Chem. Commun.* **2005**, 5647. (e) van Bommel, K. J. C.; Stuart, M. C. A.; Feringa, B. L.; van Esch, J. *Org. Biomol. Chem.* **2005**, *3*, 2917. (f) Toledano, S.; Williams, R. J.; Jayawarna, V.; Ulijn, R. V. *J. Am. Chem. Soc.* **2006**, *128*, 1070. (g) Yang, Z.; Ho, P.-L.; Liang, G.; Chow, K. H.; Wang, Q.; Cao, Y.; Guo, Z.; Xu, B. *J. Am. Chem. Soc.* **2007**, *129*, 266. (h) Engelkamp, H.; Middelbeek, S.; Nolte, R. J. M. *Science* **1999**, *284*, 785. (i) Hanabusa, K.; Maesaka, Y.; Suzuki, M.; Kimura, M.; Shirai, H. *Chem. Lett.* **2000**, 1168.

(13) Applegarth, L.; Clark, N.; Richardson, A. C.; Parker, A. D M.; Radosavljevic-Evans, I.; Goeta, A. E.; Howard, J. A. K.; Steed, J. W. *Chem. Commun.* **2005**, 5423.

(14) Stanley, C. E.; Clarke, N.; Anderson, K. M.; Elder, J. A.; Lenthall, J. T.; Steed, J. W. *Chem. Commun.* **2006**, 3199.

(15) Gale, P. A. *Acc. Chem. Res.* **2006**, *39*, 465.

(16) See, for example: (a) Kavallieratos, K.; de Gala, S. R.; Austin, D. J.; Crabtree, R. H. *J. Am. Chem. Soc.* **1997**, *119*, 2325. (b) Wisner, J. A.; Beer, P. D.; Drew, M. G. B. *Angew. Chem., Int. Ed.* **2001**, *40*, 3606. (c) Wisner, J. A.; Beer, P. D.; Berry, N. G.; Tomapatanaget, B. *Proc. Natl. Acad. Sci. U.S.A.* **2002**, *99*, 4983. (d) Wisner, J. A.; Beer, P. D.; Drew, M. G. B.; Sambrook, M. R. *J. Am. Chem. Soc.* **2002**, *124*, 12469. (e) Curiel, D.; Beer, P. D.; Paul, R. L.; Cowley, A.; Sambrook, M. R.; Szemes, F. *Chem. Commun.* **2004**, 1162. (f) Sambrook, M. R.; Beer, P. D.; Wisner, J. A.; Paul, R. L.; Cowley, A. R.; Szemes, F.; Drew, M. G. B. *J. Am. Chem. Soc.* **2005**, *127*, 2292. (g) Sambrook, M. R.; Beer, P. D.; Lankshear, M. D.; Ludlow, R. F.; Wisner, J. A. *Org. Biomol. Chem.* **2006**, *4*, 1529. (h) Chmielewski, M. J.; Jurczak, J. *Chem.−Eur. J.* **2006**, *12*, 7652.

(17) Meyer, H.; Steiner, K. *Monatsh. Chem.* **1914**, *35*, 391.

(18) (a) Lawton, E. A.; McRitchie, D. D. *J. Org. Chem.* **1959**, *24*, 26. (b) Imai, Y. *Polym. Lett.* **1970**, *8*, 555. (c) Saini, A. K.; Carlin, C. M.; Patterson, H. H. *J. Polym. Sci., Part A: Polym. Chem.* **1992**, *30*, 419. (d) Kaupp, G.; Schmeyers, J.; Boy, J. *Tetrahedron* **2000**, *56*, 6899. (e) Watson, K. G.; Cameron, R.; Fenton, R. J.; Gower, D.; Hamilton, S.; Jin, B.; Krippner, G. Y.; Luttick, A.; McConnell, D.; MacDonald, S. J. F.; Mason, A. M.; Nguyen, V.; Tucker, S. P.; Wu, W.-Y. *Bioorg. Med. Chem. Lett.* **2004**, *14*, 1589.

(19) (a) van Bommel, K. J. C.; van der Pol, C.; Muizebelt, I.; Friggeri, A.; Heeres, A.; Meetsma, A.; Feringa, B. L.; van Esch, J. H. *Angew. Chem., Int. Ed.* **2004**, *43*, 1663. (b) de Loos, M.; Friggeri, A.; van Esch, J. H.; Kellogg, R. M.; Feringa, B. L. *Org. Biomol. Chem.* **2005**, *3*, 1631.

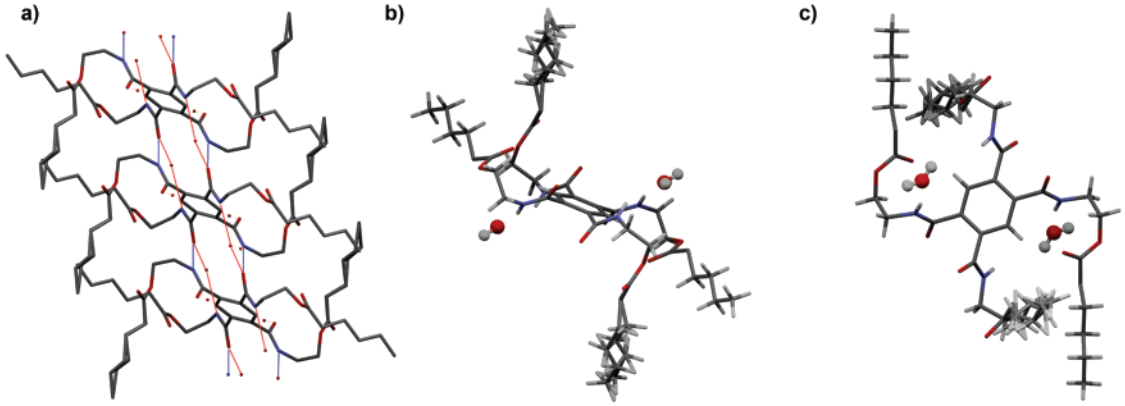

Figure 1. (a) X-ray crystal structure of **1** showing in blue (direct) and red (indirect, by water molecule) the intermolecular hydrogen-bonding network that results in one-dimensional offset stacks (hydrogen atoms have been removed for clarity). (b) Side and (c) top views of the two possible anion-binding sites, each occupied by a water molecule within the crystal structure.

Table 1. Solvents Forming a Gel with Pyromellitamide **1**

solvent[a]	min % (w/w)	T_g (°C)
hexane	1.3	45
cyclohexane	1.0	42
diethyl ether	9.7	N/A
toluene	10.0	46

[a] Solvents tested that did not form a gel included water, acetonitrile, dimethyl sulfoxide, chloroform, dichloromethane, methanol, ethanol, and 1-butanol.

aminolysis of *N*,*N*′-hydroxyethyl pyromellitimide **3**,[20] giving the pyromellitamide tetraethanol **4** that was then coupled to hexanoyl chloride to give **1** in an overall 55% yield in two steps (Scheme 1).

An X-ray crystal structure of pyromellitamide **1** was obtained from a crystal grown by slow evaporation of a 1-butanol solution of **1** (see Supporting Information for details). The crystal structure (Figure 1) shows that each molecule is in contact with six water molecules. The pyromellitamide molecules are aligned in one-dimensional columnar stacks. Two water molecules occupy sites similar to the anion binding site in Crabtree's isophthalamide-based anion receptor.[7a,16a] The other four water molecules form hydrogen-bonding bridges between adjacent columnar stacks in the crystal (Figure 1a).

Study of Gelation and Aggregation in Solution. The formation of gels from LMOG is thought to proceed from the self-assembly of columnar stacks, helical ribbons, and similar one-dimensional aggregates which then form a dense three-dimensional network encapsulating the solvent and forming a gel.[8] The crystal structure of pyromellitamide **1** shows one-dimensional columnar stacks, indicating it is a good candidate for the formation of gels in the appropriate solvent. Gel formation was studied by dissolving pyromellitamide **1** in various solvents by heating and sonication, followed by slow cooling (Table 1).

Freshly prepared samples of a hexane gel from **1** were analyzed using XRD. The XRD pattern (Figure 2) shows two closely spaced intense peaks at $2\theta = 4.30°$ and 4.72°, corresponding to a *d* spacing of 20.5 and 18.7 Å, respectively. These peaks match well with the calculated[21] (001) reflection from the solid-state structure of **1**. A second set of three peaks around

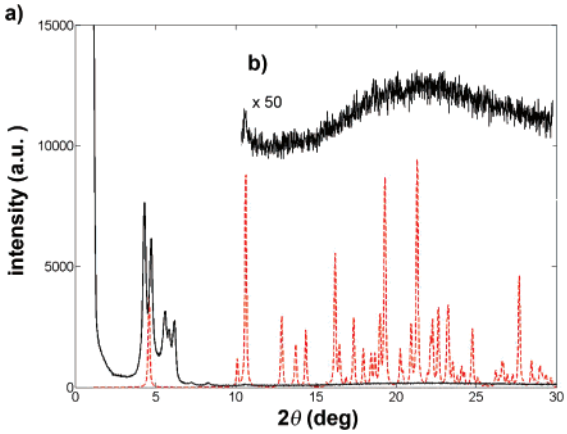

Figure 2. (a) XRD pattern obtained of a gel from pyromellitamide **1** in hexane (black solid line) compared to the calculated[21] XRD pattern (red broken line) from the single-crystal X-ray structure in Figure 1. (b) Enlargement (× 50) of the gel pattern in the 2θ range of 10−30°. The gel was loaded directly onto the sample holder, and scans were carried out immediately.

$2\theta \approx 6°$ corresponds to a *d* spacing of ca. 14−16 Å; however, this does not match with any of the reflections calculated from the solid-state structure. A very small peak at $2\theta = 10.54°$ aligns well with the (110) reflection and the smaller (010) reflections calculated in the solid-state structure at $2\theta = 10.62°$ and 10.12°, respectively. The *d* spacing values for the hexane gel from **1** obtained by XRD are consistent with one-dimensional stacks with similar dimensions as in the solid-state structure (Figure 1) but where the intercolumnar distance has been increased from ca. 9 to 15 Å.

The microstructure of the gels formed was also studied using field emission gun scanning electron (FEG-SEM), transmission electron (TEM), and atomic force (AFM) microscopy. The TEM micrograph of a dried diluted solution of pyromellitamide **1** in hexane deposited on amorphous carbon shows twisted fibers (Figure 3a and Figures S1−S3 in Supporting Information). These twisted fibers may be related to helical ribbons that have previously been reported as possible precursor structures to the formation of a gel from LMOG.[8d,f,22] The AFM (see

(20) This compound has been previously reported: Cowan, J. A.; Sanders, J. K. M. *J. Chem. Soc., Perkin Trans. 1* **1985**, 2435. See Supporting Information for experimental details for the synthesis of **3**.

(21) Calculated using *Mercury*, Crystal Structure Visualisation and Exploration software (http://www.ccdc.cam.ac.uk/free_services/mercury/), see: Macrae, C. F.; Edgington, P. R.; McCabe, P.; Pidcock, E.; Shields, G. P.; Taylor, R.; Towler, M.; van de Streek, J. *J. Appl. Crystallogr.* **2006**, *39*, 453.

(22) Díaz, N.; Simon, F.-X.; Schmutz, M.; Rawiso, M.; Decher, G.; Jestin, J.; Mésini, P. J. *Angew. Chem., Int. Ed.* **2005**, *44*, 3260.

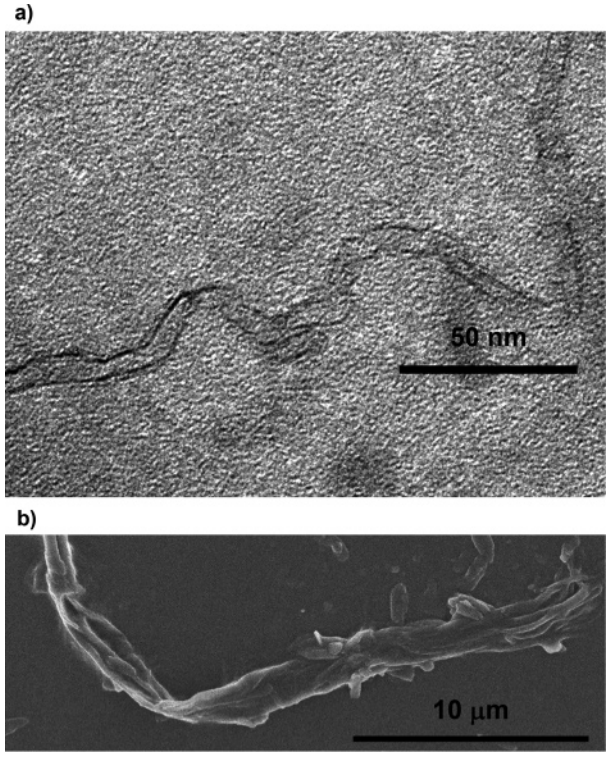

Figure 3. Micrographs of pyromellitamide **1** gels. (a) TEM image of a dried dilute hexane solution of **1** deposited on a carbon-coated Cu grid. (b) FEG-SEM of **1** cyclohexane gel, dried on a carbon tape, platinum-coated.

Figure S4 in Supporting Information) and FEG-SEM (Figure 3b) micrographs from the dried gel show various twisted fibers and bundles of fibers as is commonly reported for LMOG gels.[8,22]

The pyromellitamide **1** gels only nonpolar, aprotic solvents, forming organogels and not hydrogels.[8] This observation and XRD data above support the hypothesis that it is the same or similar hydrogen-bonding network observed in the crystal structure for **1** (Figure 1) that generates the supramolecular stacks responsible for the gel structure.

Further evidence for the key role that intermolecular hydrogen-bonding plays in the formation of gels from pyromellitamide **1** comes from FT-IR spectroscopy studies (Table 2).

The FT-IR spectral data (entry 2) for the amide groups for the cyclohexane solution of **1** (at a concentration well below the gelation point) is almost identical to the solid-state spectrum (entry 1), indicating similar hydrogen-bonding interactions in cyclohexane. In contrast, the IR spectrum of **1** in chloroform (entry 3) shows two peaks for the N−H stretch, one similar to the solid state and cyclohexane spectra at 3261 cm^{-1}, but the other peak is blue-shifted to 3431 cm^{-1}, characteristic of non-hydrogen-bonded amide groups. In $(CH_3)_2SO$, only two peaks above 3400 cm^{-1} (entry 4) are observed, indicating that there are no intermolecular hydrogen-bonding interactions in $(CH_3)_2$-SO. The data for the amide I (C═O stretching) and amide II (N−H in-plane bending coupled to a C−N stretch) peaks show that the former is blue-shifted in $(CH_3)_2SO$ and slightly red-shifted in chloroform, while the latter is red-shifted in both $(CH_3)_2SO$ and chloroform compared to the solid state and cyclohexane solution spectra. This is consistent with a decrease in intermolecular hydrogen bond driven aggregation[23] of **1** in the order solid state > cyclohexane > chloroform > $(CH_3)_2$-SO.

The hydrogen bond driven intermolecular aggregation of pyromellitamide **1** was also evident from a comparison of the ^1H NMR spectra of **1** in various solvents (Figure 4a−c). Here, a similar trend appears as from the FT-IR solution data; in $CDCl_3$ the "core" amide (δN−H) and aromatic (δAr−H) proton resonances are very broad compared to the same peaks in d_6-acetone, which in turn are broader than those observed in d_6-$(CH_3)_2SO$. It is also noteworthy that, in both $CDCl_3$ and d_6-acetone, the proton resonances corresponding to the hexanoyl side chain are significantly sharper than the δN−H and δAr−H, in line with the rigid core/flexible tail model mentioned above. In d_{12}-cyclohexane, even at elevated temperatures, the spectrum (not shown) was too broad to resolve any peaks, indicating that the degree of aggregation for **1** is greater than in any of the other solvents shown in Figure 4. Given this and the broadness of the $CDCl_3$ spectrum, we decided to focus on d_6-acetone to study the aggregation of **1** in more details. When plotted against increasing concentration of **1**, the ^1H NMR data in d_6-acetone (Figure 4e) show significant downfield and upfield shifts, for the δN−H and δAr−H, respectively.

The δN−H downfield shift in Figure 4e is consistent with an increase in intermolecular hydrogen bonding as the concentration of **1** increases. The upfield shift for δAr−H suggests co-facial stacking of **1** in the aggregates formed, possibly similar to that observed in the single-crystal X-ray structure (Figure 1). We fitted the data to three different aggregation models (Figure 5): a simple 1:1 dimerization (Dim)[24,25] and both the simple noncooperative Equal K model (EK) and its cooperative version (coEK) described by Martin.[25]

The best fit for the aggregation of **1** in d_6-acetone was obtained with the coEK model, giving $K_E = 232\ M^{-1}$ and $\rho = 0.22$ (corresponding to $K_2 = 51\ M^{-1}$). The goodness of fit as judged by comparing the chi squared (χ^2) and the covariance of the fit (cov_{fit})[26] for the coEK model was an order of magnitude better than either the noncooperative EK model or the simple dimerization. According to the coEK model,[25] when $\rho < 1$, as observed here, it indicates that the formation of the dimer **1**/**1** is more difficult than subsequent addition of **1** to a growing stack (i.e., the aggregation of **1** is positively cooperative). This could be simply due to favorable entropy for aggregation as a dimer formation will lead to some loss of orientational freedom while addition of another molecule of **1** to the growing aggregate involves only the loss of entropy of one monomer.[25,27] In our case, the well-known cooperative hydrogen-bonding effect,[28] where neighboring protic groups increase the strength of hydrogen bonds, undoubtedly plays a role as well.

(23) Miyazawa, T.; Shimanouchi, T.; Mizushima, S.-I. *J. Chem. Phys.* **1956**, *24*, 408.
(24) Connors, K. A. *Binding Constants*; Wiley & Sons: New York, 1987.
(25) Martin, R. B. *Chem. Rev.* **1996**, *96*, 3043.
(26) The covariance of the fit (cov_{fit}) is calculated by dividing the covariance of the residual (raw − calculated data) with the covariance of the raw data. This value is independent of the number of variables but reflects the distributions of the residuals; the lower the cov_{fit} value, the better the fit.
(27) Sarolea-Mathot, L. *Trans. Faraday Soc.* **1953**, *49*, 8.
(28) (a) Allen, F. H.; Kennard, O.; Taylor, R. *Acc. Chem. Res.* **1983**, *16*, 146. (b) Guo, H.; Karplus, M. *J. Phys. Chem.* **1994**, *98*, 7104. (c) Schneider, H.-J.; Yatsimirsky, A. *Principles and Methods in Supramolecular Chemistry*; Wiley & Sons: Chichester, 2000.

Table 2. Selected Data for the Amide Peaks from FT-IR Spectra of Pyromellitamide **1** (Entries 1−4) and Its Corresponding TBA−Br Complexes (Entries 5−7)

entry	sample	νN–H (cm^{-1})	amide I (cm^{-1})	amide II (cm^{-1})
1	**1** (thin film)	3242	1635	1566
2	**1** (1 mM in cyclohexane)	3253	1635	1558
3	**1** (1 mM in $CHCl_3$)	3431, 3261[a]	1622	1533
4	**1** (1 mM in $(CH_3)_2SO$)	3440, 3496[a]	1667	~1540[b]
5	**1** + 10 equiv of TBA−Br (thin film)	3211	1662	1537
6	**1** + 10 equiv of TBA−Br (1 mM in $CHCl_3$)	3392, 3211[a]	1658	1544
7	**1** + 1 equiv of TBA−Br (1 mM in cyclohexane)	3443, 3315, 3156[c]	1684, 1635[a]	1533

[a] These peaks have similar intensities. [b] This peak is extremely weak, broad (1510−1570 cm^{-1}), and partially obscured by a large solvent peak. [c] These peaks are very broad and overlap each other.

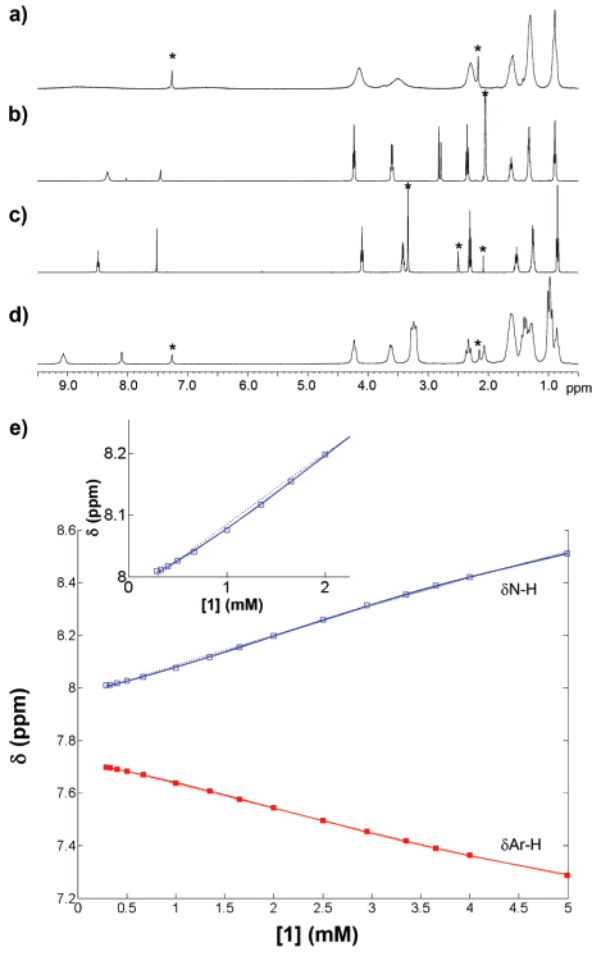

Figure 4. ^{1}H NMR spectra at 300 K of **1** in (a) $CDCl_3$ (200 MHz), (b) d_6-acetone (400 MHz), (c) d_6-$(CH_3)_2SO$ (400 MHz), and (d) $CDCl_3$ with 2.0 equiv of TBA−Cl added (200 MHz). In all these spectra, the residual water, acetone, $(CH_3)_2SO$, and $CHCl_3$ resonances are indicated with an asterisk (*). (e) ^{1}H NMR (400 MHz, d_6-acetone) at 300 K of the δN−H (blue open squares) and δAr−H (red solid circles) of pyromellitamide **1** at different concentrations of **1**. Also shown are the calculated aggregation isotherms for the cooperative (coEK, solid line) and noncooperative (EK, broken lines) Equal K aggregation models, the latter also equal to the simple dimerization (Dim) model. The insert in the top left corner of (e) shows an enlargement of the region between 0 and 2 mM for the δN−H. See text for details.

Anion Binding. According to earlier work, isophthalamide receptors bind anions between the two amide N−H's.[7a,16a] In the X-ray structure of pyromellitamide **1**, these potential binding sites are co-occupied by a carbonyl of an adjacent **1** and a water molecule (Figure 1b,c). The two isophthalamide sites in **1** are in a chair conformation with respect to each other (Figure 1b).

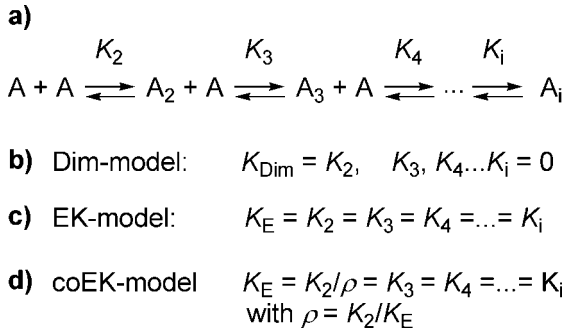

Figure 5. (a) Successive equilibria for self-association of molecule A and the three models (b−d) used here fit the data for the aggregation of **1**. The factor ρ in (d) describes the cooperativity of aggregation with $\rho < 1$ positive cooperativity for aggregation vs dimerization, $\rho = 1$ no cooperativity (same as EK-model in c), and $\rho > 1$ negative cooperativity for aggregation vs dimerization. See ref 25 and text for details.

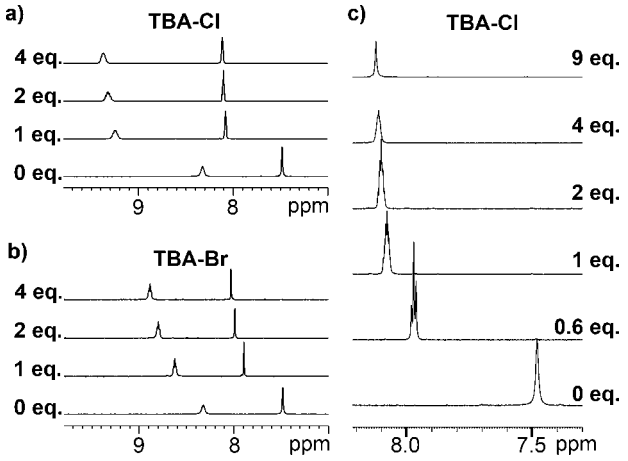

Figure 6. ^{1}H NMR spectra (400 MHz, d_6-acetone) from titration experiments with (a) TBA−Cl and (b) TBA−Br added to pyromellitamide **1**. The resonances shown are the δN−H (amide, right) and δAr−H (aromatic proton, left). (c) A more detailed view of the δAr−H resonances upon the addition of TBA−Cl to **1**. The numbers of equivalents added are indicated on the left (a, b) or right (c) of the spectra.

To explore the anion binding and the interaction between these sites in **1**, we titrated it with tetrabutylammonium (TBA^+) salts of chloride (Cl^-), bromide (Br^-), iodide (I^-), nitrate (NO_3^-), acetate (OAc^-), and hexafluorophosphate (PF_6^-) and monitored the binding by ^{1}H NMR in d_6-acetone. Titration of **1** with TBA−Cl causes the aromatic and amide host resonances to shift downfield (Figure 6a). Titration with TBA−Br causes similar but less pronounced shifts, indicating weaker binding (Figure 6b). For TBA−I and TBA−NO_3, these shifts are smaller still, while TBA−OAc causes even larger shifts than TBA−Cl. No

Table 3. Apparent Association Constants K_a for the Complexation of **1** toward Various Anions (as TBA Salts) Obtained from NMR Titrations in d_6-Acetone at 300 K[e]

	1:1 binding model		1:2 binding model			
anion	K_a (M^{-1})[a]	cov_{fit} ($\times 10^3$)[b]	K_{1a} (M^{-1})[a]	K_{2a} (M^{-1})[a]	α[c]	cov_{fit} ($\times 10^3$)[b]
Cl^-	71000	4.0	data could not be fitted[d]			
Br^-	1100	2.6	14000	430	0.12	3.6
I^-	92	2.3	420	40	0.38	1.7
NO_3^-	130	1.5	460	70	0.61	0.1
OAc^-	1300	2.9	120000	200	0.007	0.6

[a] Estimated errors: 50%. [b] See ref 26. [c] Interaction cooperativity parameter: see refs 24 and 30. [d] The data could not be fitted to a realistic 1:2 binding model (K_{1a} and $K_{2a} \gg 10^7$, $cov_{fit} = 20 \times 10^{-3}$). [e] Results for both a 1:1 and 1:2 binding models are shown. The concentration of **1** is in each case fixed at 2−3 mM. See text for details.

significant chemical shifts are observed in the ^{1}H NMR of pyromellitamide **1** after adding excess TBA−PF_6, demonstrating that only relatively small anions can bind to **1** and that the TBA cation has no effect on **1**. These results are consistent with earlier anion binding studies on other isophthalamide receptors. The binding of anions to **1** is not limited to d_6-acetone; in deuterated chloroform the broad resonances for **1** (due to aggregation) get significantly sharper upon the addition of TBA−Cl (compare parts a and d of Figure 4).

Detailed analysis of the binding data and the stoichiometry of binding was complicated by the fact that **1** aggregates in d_6-acetone. Attempts to determine stoichiometry by the Job plot method failed (see Supporting Information), as the changes in δN−H and δAr−H at different concentrations of **1** (Figure 4e) either add to or counteract the chemically induced shifts of δN−H and δAr−H caused by additions of anions. This causes the Job plot to show different outcomes for the δN−H and δAr−H, making it impossible to use to determine stoichiometry. To overcome the problem with the aggregation of **1**, we performed all the anion titrations at a constant concentration of **1** (as described in Supporting Information). At the concentrations used in our experiments (2−3 mM), we calculated that 65−75% of **1** is in the monomer state, on the basis of the data we obtained from the coEK model (Figure 5). We tried to fit the data to binding models that take aggregation of the host into account,[29] but due to large numbers of independent parameters in the binding equation, no sensible results could be obtained. We then fitted the data to classical 1:1 and 1:2 binding models,[24] ignoring the effect of aggregation of **1** (Table 3).

Our results suggest that the binding data fit better to a 1:2 binding model. The only apparent exception to this in Table 3 is Cl^-, which could not be fitted to a 1:2 model but that is probably because the association constants are too high to be determined from NMR data (aside from the complications arising from aggregation of **1**). The strongest evidence for 1:2 binding, however, comes from breaking of the symmetry of the δAr−H (Figure 6c) upon addition of 1 equiv of Cl^-. The symmetry of the δAr−H is then gradually restored as more Cl^- is added, which is expected as **1** binds to the second anion. This data also suggest that the relative strength of anion binding to **1** decreases in the order $Cl^- > OAc^- > Br^- > NO_3^- \approx I^-$, which is in good agreement with earlier work on the related isophthalamides.[7a,15,16]

The symmetry breaking for Cl^- and the calculated (apparent) 1:2 association constants for the other anions in Table 3 suggest that **1** displays negative cooperativity toward anions as the interaction cooperativity parameter[26,30] ($\alpha = 4K_{2a}/K_{1a}$) is always less than 1. This negative cooperativity appears to be allosteric in nature (i.e., due to reversible discrete conformational changes in the host that take place in the first binding event).[1,6] Using the nomenclature of Crabtree,[7a] we find that the isophthalamide binding site must adopt a (syn−syn) orientation to bind the first anion (Figure 7). To bind a second anion, the amide groups of the opposite binding site must adopt the same conformation, resulting in an overall (syn−syn)−(syn−syn) conformation for **1** in which there would be some electronic repulsion between amide−carbonyl oxygen lone pairs. If the empty binding site was to adopt an (anti−anti) or an (anti−syn) conformation, however, it cannot bind to the second anion but instead hydrogen bonds are formed to the carbonyl of the (first) occupied anion-binding site. These conformers would be more stable than the (syn−syn) conformer required for anion binding, resulting in the observed negative cooperativity for the second binding event. Simple molecular modeling studies (Hyperchem[31] − MM+ force field) on the three uncomplexed conformers in Figure 7 support this explanation: the di-destabilized (syn−syn)−(anti−anti) conformer is 29 kJ mol^{-1} and the monostabilized (syn−syn)−(syn−anti) is 9 kJ mol^{-1} higher in energy than the distabilized (syn−syn)−(anti−anti) conformer. In comparison, the energy penalty[6a,b] for the second anion binding to **1** is 2−12 kJ mol^{-1} on the basis of the data in Table 3.

Effect of Anions on Gel Formation and Stability. Addition of as little as 0.25 equiv of TBA−Cl or TBA−Br to pyromellitamide **1** in cyclohexane, under the same conditions as in Table 1, was enough to inhibit the formation of a gel. Addition of TBA−PF_6 (1 equiv) did not affect the ability of **1** to form a gel. Adding these salts to preformed **1** cyclohexane gels had the same effect on their stability (i.e., TBA−Cl and TBA−Br caused the gels to collapse whereas TBA−PF_6 did not). The complete gel disruption by TBA−Cl and TBA−Br depended on the mixing efficiency; if the gel was sonicated briefly after adding the salts it collapsed almost instantaneously, while it took from a few tens of seconds to several minutes for the gel to collapse when the salts were simply placed on top of the gel. Other TBA−salts, including TBA−I, TBA−OAc, and TBA−NO_3, had a similar effect. It is noteworthy that the time it takes for anions to collapse the gel correlates qualitatively with the anion strength reported above (Table 3) in the order $Cl^- > AcO^- > Br^- > NO_3^- > I^-$, with the TBA−Cl salt causing the quickest collapse (within few tens of seconds) and TBA−I the slowest (up to 1 h). The solubility of the anion in the gelating solvent also plays a role. Adding an aqueous solution of NaCl did not disrupt the gels, instead a phase separation was observed just as in the case of pure water and **1** cyclohexane gels.

The ability of anions to inhibit and destabilize the gelation of **1** in nonpolar solvent is in line with NMR studies in deuterated chloroform and acetone (Figures 4a,d and 6). The FT-IR data in Table 2 (entries 5−7) also show that anions destabilize the hydrogen-bonding network that drives the aggregation of **1**. The data for the solid-state complex between

(29) (a) Steiner, R. F. *J. Theor. Biol.* **1974**, *45*, 93. (b) Wolfer, G. K., Jr.; Neil, J. L.; Rippon, W. B. *J. Protein Chem.* **1987**, *6*, 441.
(30) Connors, K. A.; Paulson, A.; Toledo-Velasquez, D. T. *J. Org. Chem.* **1988**, *53*, 2023.
(31) *Hyperchem* 6.03; Hypercube, Inc.: Gainesville, FL, 2000.

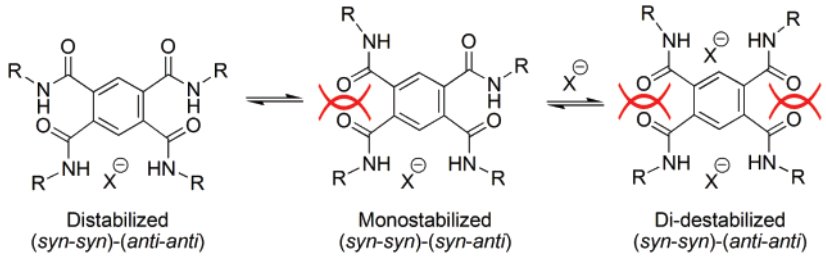

Figure 7. Three different conformers that pyromellitamide **1** can adopt after binding to a single anion. Only the least stable conformer on the right is capable of binding another anion. See text for details.

1 and TBA−Br (compare entries 1 and 5 in Table 2) show a red shift of both the N−H stretch and the amide II peaks and blue shift for the amide I peaks. Similar trends are also observed in chloroform and cyclohexane solutions, suggesting the destabilizing effects of TBA−Br are the same in these solvents and the solid state.

Conclusions

Pyromellitamide **1** forms aggregates by a one-dimensional intermolecular hydrogen-bonding network similar to that observed in the single-crystal X-ray structure of **1**. In nonpolar solvents such as hexane, the aggregation is strong enough for **1** to form gels. In deuterated acetone, where **1** does not aggregate as strongly, the NMR dilution data could be fitted to the cooperative equal K (coEK) aggregation model with positive cooperativity.

Pyromellitamide **1** also binds to a range of small anions with similar selectivity as observed for other isophthalamides. The host **1** has two potential anion-binding sites, and although the data analysis is complicated by the aggregation of **1**, we conclude that **1** can indeed bind two anions, albeit with negative cooperativity. The NMR and IR study of anion complexation with **1** clearly indicates that these anions interfere and disturb the hydrogen-bonding network that is responsible for the aggregation of **1**. This is not surprising as these anions bind to the same amide groups in **1** that are responsible for its aggregation. The ability of anions to act as a stimuli for the dissociation of **1** was then demonstrated on gels from **1**. The stimuli-response time for the dissociation of cyclohexane gels from **1** was qualitatively correlated to the measured binding strength of **1** in deuterated acetone. This suggests that the anion sensitivity of gels formed from **1** might find applications in anion sensors and release systems for biomedical applications. To realize these applications and explore the gelating and anion properties of pyromellitamides, we are currently synthesizing a range of these compounds, including compounds that could form gels in water.

Experimental Section

General Remarks. Details of equipment and techniques used, including binding and microscopy studies, and the synthesis of the previously reported[20] compound **3** are given in the Supporting Information.

***N,N′,N″,N‴*-1,2,4,5-Tetra(hydroxyethyl) Pyromellitamide (4).** Diimide **3** (0.10 g, 0.3 mmol) was suspended in ethanol (6 mL) at 60 °C, and 2-aminoethan-1-ol (0.17 g, 2.8 mmol) added. The diimide **3** gradually dissolved, after which a fine white precipitate formed. After 30 min, the reaction was filtered and washed with ethanol, yielding **3** (0.08 g, 62%) as a fine white powder: mp 197−198 °C; ^{1}H NMR (d_6-$(CH_3)_2SO$, 200 MHz) δ 3.26 (m, 8H), 3.50 (m, 8H), 4.65 (t, J = 5.7 Hz, 4H), 7.57 (s, 2H), 8.29 (t, J = 5.6 Hz, 4H); ^{13}C NMR (d_6-$(CH_3)_2SO$, 75.4 MHz) 42.0, 59.5, 127.0, 136.5, 167.1; FTIR (KBr, cm^{-1}) 3404 (s), 3242 (s), 3080 (m), 2927 (m), 2869 (m), 1627 (s), 1556 (s), 1315 (s), 1068 (s); *m/z* HRMS (ESI) calcd for $C_{18}H_{26}N_4O_8$ ([M + H]$^+$) 427.1829, found 427.1822. Anal. Calcd for $C_{18}H_{26}N_4O_8$ (426.421): C 50.70, H 6.15, N 13.14. Found C 50.82, H 6.15, N 13.16.

***N,N′,N″,N‴*-1,2,4,5-Tetra(ethylhexanoate) Pyromellitamide (1).** Compound **4** (0.35 g, 0.82 mmol) was added to acetonitrile (25 mL) with pyridine (0.47 g, 5.9 mmol) and 4-dimethylaminopyridine (0.080 g, 0.65 mmol). To this was added hexanoyl chloride (0.82 g, 6.1 mmol). After 1 h, all solid material had dissolved, and the solution was then stirred overnight at room temperature. The reaction mixture was then poured onto an ice−water slurry (30 g) and stirred for 1 h. The product was then extracted into dichloromethane (50 mL), washed with saturated sodium bicarbonate (2 × 50 mL) and water (50 mL), dried over anhydrous magnesium sulfate, filtered, and evaporated to dryness to yield **1** (0.56 g, 88%) as a pastelike material that hardened slightly after drying: mp 115 °C; ^{1}H NMR (d_6-$(CH_3)_2SO$, 400 MHz) δ 0.85 (t, J = 6.8 Hz, 12H) 1.25 (m, 16H), 1.53 (m, 8H), 2.30 (t, J = 7.5 Hz, 8H), 3.42 (m, 8H), 4.10 (t, J = 5.9 Hz, 8H), 7.52 (s, 2H), 8.48 (t, J = 5.9 Hz, 4H); ^{13}C NMR (d_6-$(CH_3)_2SO$, 50.3 MHz) 13.8, 21.8, 24.0, 30.7, 33.4, 40.8, 62.1, 127.1, 136.7, 167.2, 173.0; FTIR (thin film, cm^{-1}) 3242 (s), 3072 (s), 2956 (d), 2860 (d), 1741 (s), 1635 (s), 1566 (s), 1168 (s); *m/z* HRMS (ESI) calcd for $C_{42}H_{66}N_4O_{12}$ ([M + Na]$^+$) 841.4570, found 841.4559. Anal. Calcd for $C_{42}H_{66}N_4O_{12}$ (818.468): C 61.59, H 8.12, N 6.84. Found C 61.57, H 8.25, N 6.94.

Gel Formation: The Inversion Test. In a typical experiment, a weighed amount of **1** and the solvent (1.0 mL) were placed in a vial. When applicable, 0.25−1.0 equiv of the TBA−anion salt was also added to this vial. The vial was heated around the boiling point of the solvent being tested until the mixture turned into a clear solution. The solution was allowed to cool slowly to room temperature, and the vial with a closed lid was inverted to determine whether the solution was completely immobilized to achieve gelation.

Determination of Gelation Temperature (T_g). In a typical experiment, the vial containing a gel was immersed inversely in a water bath while the temperature was raised slowly. T_g was determined as the temperature at which the gel collapses such that the gel was no longer immobilized according to the inversion test described above.

Anion-Induced Gel Collapse. To a preformed gel of typically 1.5% (w/w) of **1** in cyclohexane, 1 equiv of the TBA−anion salt was added to the surface and allowed to diffuse through the gel. The time taken for the gel → sol transition was then measured by periodically testing the gel by the inversion test. Due to the hygroscopic nature of TBA−OAc, the entire system was contained under an atmosphere of nitrogen.

Acknowledgment. We acknowledge the financial support of the Australian Research Council (ARC), including an APAI scholarship to J.E.A.W. from an ARC Linkage Grant (LP0455238) to M.J.C. and P.T. and a Discovery Project Grant and an

Australian Research Fellowship (DP0666325) to P.T. The University of Sydney is thanked for providing a Sesqui Postdoctoral Research Fellowship to P.T. We thank the staff in the NANO Major National Research Facility at the Electron Microscope Unit, The University of Sydney, particularly Tony Romeo and Emine Korkmaz, for help with FEG-SEM studies.

Supporting Information Available: Details of equipment and techniques used, synthesis of **3**, methodology for binding studies and binding models used, Job plot, AFM images, NMR spectra of **1**, and details for single-crystal X-ray diffraction analysis of **1**. This material is available free of charge via the Internet at http://pubs.acs.org.

JA0713781